Journal of Alloys and Compounds 685 (2016) 587–592

Contents lists available at ScienceDirect

Journal of Alloys and Compounds

journal homepage: http://www.elsevier.com/locate/jalcom

Phase transformations and aging of the $Cu_{72.9}Al_{15.0}Mn_{10.5}Ag_{1.6}$ alloy

C.M.A. Santos [a], A.T. Adorno [a], N.Y. Oda [b], B.O. Sales [b], L.S. Silva [b], R.A.G. Silva [b, *]

[a] Departamento de Físico-Química, Instituto de Química, UNESP, Caixa Postal 355, 14801-970 Araraquara, SP, Brazil
[b] Departamento de Ciências Exatas e da Terra, UNIFESP, 09972-270 Diadema, SP, Brazil

ARTICLE INFO

Article history:
Received 16 April 2016
Received in revised form
27 May 2016
Accepted 28 May 2016
Available online 29 May 2016

Keywords:
Metals and alloys
Solid state reactions
Kinetics

ABSTRACT

The phase transformations and aging of the $Cu_{72.9}Al_{15.0}Mn_{10.5}Ag_{1.6}$ alloy were studied in the temperature range from 523 to 723 K using measurement of change in microhardness with variation in quenching temperature and aging time, differential scanning calorimetry (DSC), X-ray diffractometry (XRD), magnetization measurements with temperature and applied field, optical microscopy (MO) and high-resolution transmission electron microscopy (HRTEM). The results indicated that the bainitic precipitation is dominant with increase in microhardness and the activation energy value obtained for this process is lower than that reported in the literature due to the occurrence of a diffusion process disturbed by the presence of Ag dissolved in the alloy.

1. Introduction

The Cu-based shape memory alloys (SMAs) are the most attractive alloys for practical applications because of their low cost and relatively good SM properties [1]. The shape memory properties in Cu-based alloys depend on the martensitic transformation stability, and therefore, they also depend on the β phase stability. Precipitation of stable phases is an important and interesting phenomenon. It results in decomposition of the metastable parent phase and in turn leads to an ultimate loss of the shape memory [2]. Similar to other Cu-based shape memory alloys the CuAlMn is a commercially attractive system. Addition of Mn to the binary Cu-Al alloy results in an enhanced ductility compared with the other CuAl-based alloys [3] and makes the β phase more stable to diffusional decomposition than it is in other Cu-based alloys and slows down this decomposition when the β phase becomes metastable [4]. The degree of order in the β parent phase may decrease with decreasing Al content. Actually, in the high Al composition range (above 16 at.%Al), the ordering to the $L2_1$ structure cannot be suppressed by quenching from the disordered A2 phase region, and the $L2_1$ phase martensitically transforms into a 6 M structure with six layered modulation. However, in the low Al composition range (below 16 at.%), the ordering from the A2 to the $L2_1$ structure can be suppressed by quenching and the martensitic transformation from A2 to 2 M (A1, disordered fcc) structure occurs at low temperature. The effects of aging on the hardness, microstructure and thermoelastic martensitic transformation in CuAlMn-based shape memory alloys have already been investigated [1,5]. In general, the results have been shown that during aging of CuAlMn alloys the bainitic precipitation can occur [1] and the shape memory effect may be affected [5]. There are few results in the literature for the aging of CuAlMnAg alloys [6]. The silver addition to CuAlMn alloys may improve its corrosion resistance, microhardness and increase the fraction of ferromagnetic $L2_1$ phase, thus producing an increase in the saturation magnetization of CuAlMnAg alloys [7]. In this work, the phase transformations and aging of the $Cu_{72.9}Al_{15.0}Mn_{10.5}Ag_{1.6}$ alloy were studied using microhardness change measurements with quenching temperature and aging time, magnetization measurements with temperature and applied field, differential scanning calorimetry (DSC), X-ray diffractometry (XRD), optical microscopy (MO) and high-resolution transmission electron microscopy (HRTEM) to analyze the effects of the presence of silver on the phase transformations and bainite precipitation during aging of the alloy.

1.1. Experimental procedure

The $Cu_{72.9}Al_{15.0}Mn_{10.5}Ag_{1.6}$ alloy (at.%) was prepared in an arc furnace under argon atmosphere using 99.95% copper, 99.97% aluminum, 99.98% silver and 99.95% manganese as starting materials. The samples were annealed for 120 h at 1173 K for homogenization and after annealing they were maintained at 1173 K for 1 h and quenched in water at 273 K. The Vickers microhardness

* Corresponding author.
E-mail address: galdino.ricardo@gmail.com (R.A.G. Silva).

http://dx.doi.org/10.1016/j.jallcom.2016.05.303
0925-8388/

measurements were made with a HMV-2T SHIMADZU TESTER using a load of 9.8 N for 30 s. The microhardness of the quenched alloy was then isochronically measured as a function of quenching temperature in the range from 323 to 1123 K. The measurement of microhardness change with the aging time was made on another sample quenched from 1173 K in water at 273 K and aged in the temperature range from 523 to 723 K. Optical micrographs and X-ray diffraction pattern were obtained to identify the phases present in the alloy at different quenching temperatures and aging times. The optical micrographs were obtained using an Olympus microscope BX41M-LED. The X-ray diffraction (XRD) pattern was obtained using a Brucker D50 Advanced diffractometer, Cu Kα radiation, solid samples and rotation of 30 rpm. High-resolution transmission electron micrograph was obtained using a Philips microscope, model CM200, operating at 200 kV. The X-ray diffraction pattern was refined using the Rietveld method [8] and the TOPAS software [9] to identify and quantify the phases in the studied alloy. DSC curves were obtained at different heating rates using a DSC Q20 TA Instruments. The instrument was calibrated with high purity indium standard and the purge gas was argon with flow of 50 mL min^{-1}. Samples of about 10 mg and 3.0 mm of diameter were used in platinum crucible. The heat flow curves at different heating rates were normalized in relation to sample mass.

2. Results and discussion

Fig. 1a shows the DSC curves obtained for the $Cu_{72.9}Al_{15.0}Mn_{10.5}Ag_{1.6}$ alloy quenched from 1173 K in water at 273 K. In these curves it is possible to see two thermal events: one endothermic during heating and other exothermic during cooling. These peaks are associated with forward and reverse martensitic transformations, β(A2)⇆β′(A1) [10]. The forward martensitic transition presents critical temperatures at about 223 K (M_s) and 204 K (M_f), while reverse transformation temperatures are around 230 K (A_s) and 249 K (A_f), respectively. The hysteresis value obtained is at about 26 K. This small hysteresis is one of the typical characteristics of thermoelastic martensitic transformation [10]. This indicates that after quenching from 1173 K in water at 273 K the martensitic phase is not produced, but just α and β(A2) phases are retained as suggested in Ref. [10] and Fig. 2. This figure shows a HRTEM image of a phase that exhibits an interlayer spacing of 0.290 nm which may belong to one spacing plane for the β(A2) phase. It is important to observe that there is no information about the β(A2) phase with Im3 m space group in the literature consulted.

In Fig. 1b one can observe the microhardness change measurements with quenching temperature obtained for a sample quenched from 1173 K in water at 273 K. In this curve one can verify a hardness decrease between 323 K and 423 K due to α phase precipitation that precedes the Cu_2AlMn ($L2_1$) phase formation in the $Cu_{72.9}Al_{15.0}Mn_{10.5}Ag_{1.6}$ alloy. In the temperature range from

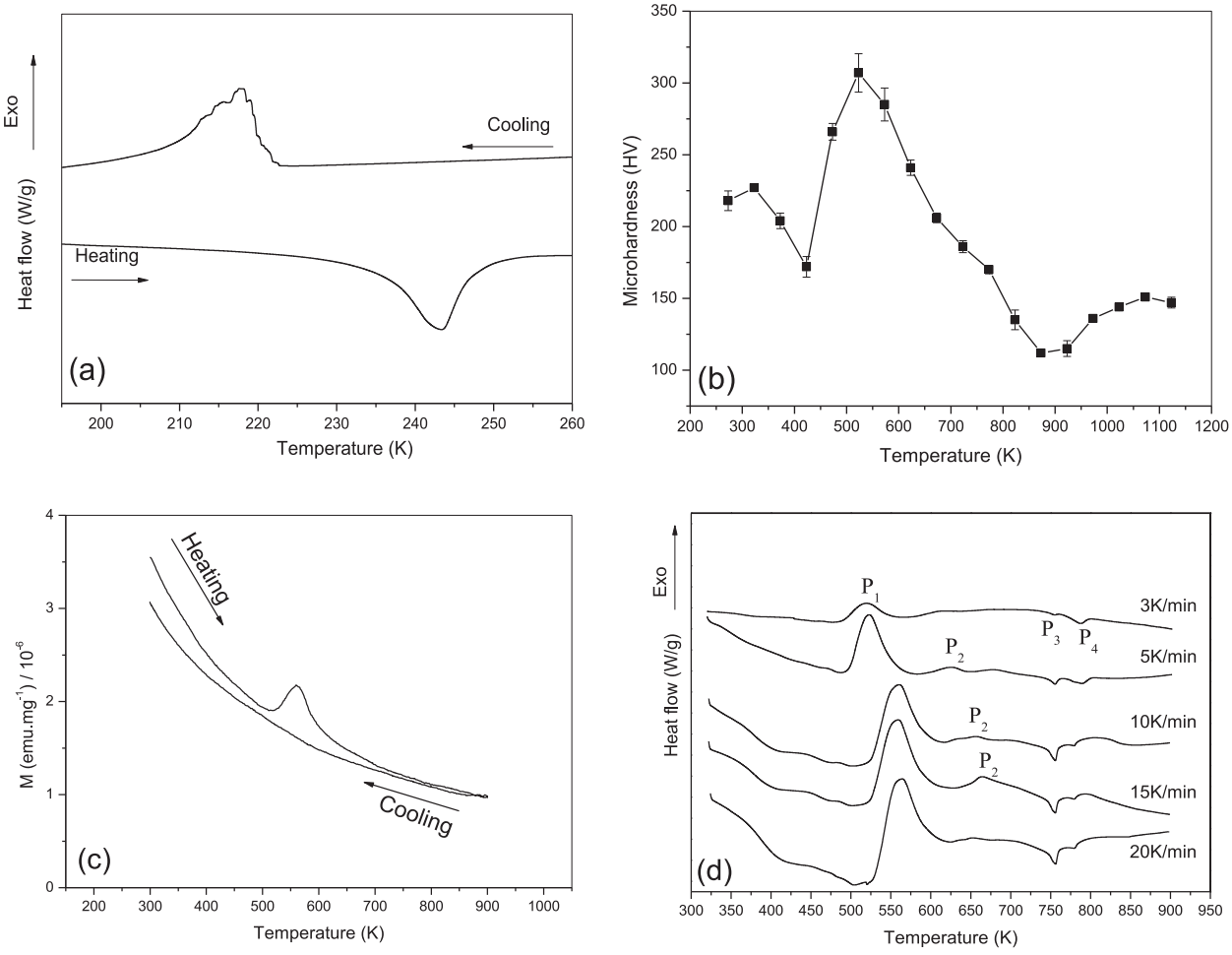

Fig. 1. (a) DSC curves obtained with a heating rate of 3.0 K/min, (b) Microhardness change measurements with quenching temperature, (c) Magnetization change vs. temperature curve, (d) DSC curves obtained in different heating rates for samples of the $Cu_{72.9}Al_{15.0}Mn_{10.5}Ag_{1.6}$ alloy initially quenched from 1173 K in water at 273 K.

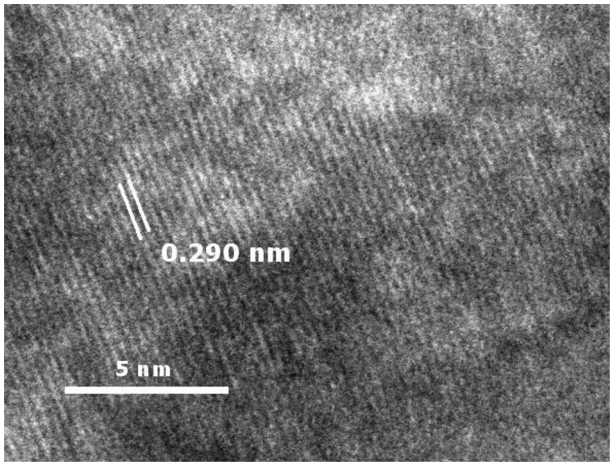

Fig. 2. HRTEM image of a phase that shows an interlayer spacing of 0.290 nm which may belong to one spacing plane for β(A2) phase. Micrograph obtained for sample quenched from 1173 K in water at 273 K.

423 K to 523 K the bainite precipitation occurs [11], thus increasing the microhardness values up to 307 HV. From 523 K to 723 K the microhardness values decrease due to the lamellae thickening of the bainitic phase, the formation of the $\beta_1(DO_3)$, T_3-Cu_3AlMn_2, α and β_{Mn} phases and precipitation of an Ag-rich phase, as seen in Fig. 3 and Table 1. From 723 K to 823 K there is an additional decrease in the microhardness values associated with the $\beta_1(DO_3)$+T_3-Cu_3AlMn_2+α+β_{Mn} + Ag_{ppt} → $\beta_2(B2)$+T_3-Cu_3AlMn_2+α reaction, followed by the T_3-Cu_3AlMn_2+α+$\beta_2(B2)$ → β(A2)+α transformation from 823 K. After 873 K the microhardness values are increased because of α phase consumption from β(A2)+α field.

Fig. 1c shows the magnetization change measurements vs. temperature obtained from a sample initially quenched from 1173 K in water at 273 K with cooling/heating rates of 10 K/min at 200 Oe. In this curve it is possible to see that during heating the magnetization values decrease with temperature and show a peak at about 560 K. This peak starts at about 500 K and is finished around 700 K. This indicates that a fraction of the ferromagnetic phase is produced between 500 K and 560 K, and then it is decomposed up to 700 K. The X-ray diffraction pattern in Fig. 3 and Table 1 show that the ferromagnetic Cu_2AlMn ($L2_1$) phase is stable in the temperature range cited. On cooling no peak was observed, but the magnetization values are increased due to the presence of Mn. Therefore, in these experimental conditions the ferromagnetic Cu_2AlMn ($L2_1$) phase is formed from the ordering of a β(A2) phase fraction produced immediately after quenching from 1173 K in water at 273 K, and then the $L2_1$ phase undergoes to paramagnetic $\beta_1(DO_3)$ structure at about 700 K. These ordering reactions are started at the final stage of the bainite precipitation at about 500 K.

In this way, during heating of the $Cu_{72.9}Al_{15.0}Mn_{10.5}Ag_{1.6}$ alloy quenched from 1173 K in water at 273 K the α phase precipitation occurs. In sequence, the bainitic phase precipitation is observed and the $\beta(A2) \rightarrow \beta_3(L2_1)_{ferromagnetic} \rightarrow \beta_1(DO_3)$ ordering reactions occur in the temperature range between 500 and 700 K. From 523 K the formation of the T_3-Cu_3AlMn_2, α and β_{Mn} phases from the β(A2) phase partial decomposition occurs together with precipitation of Ag up to around 723 K. It is interesting to notice that a fraction of the β(A2) phase is decomposed and the other is ordered, hence this phase is submitted to a set of parallel reactions from 500 K.

Fig. 1d shows the DSC curves obtained at different heating rates for samples of the $Cu_{72.9}Al_{15.0}Mn_{10.5}Ag_{1.6}$ alloy initially quenched from 1173 K in water at 273 K. The exothermic event P_1 at about 520 K is due to the bainite precipitation. In the same temperature range of peak P_1 must begin the formation of the T_3-Cu_3AlMn_2, α

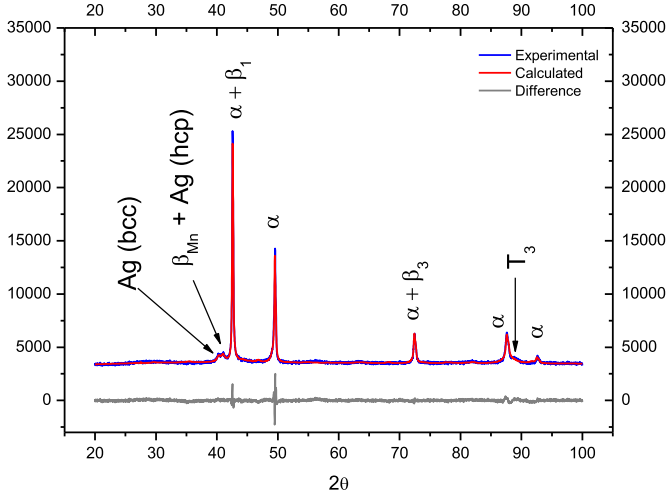

Fig. 3. X-ray diffraction pattern obtained for a sample of the $Cu_{72.9}Al_{15.0}Mn_{10.5}Ag_{1.6}$ alloy initially quenched from 1173 K in water at 273 K and then quenched again from 560 K in water at 273 K.

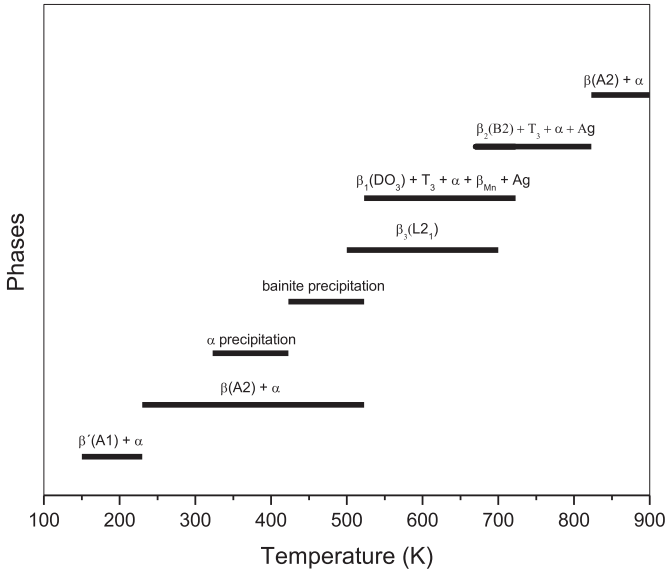

Fig. 4. Plot of stability range of phases proposed for the $Cu_{72.9}Al_{15.0}Mn_{10.5}Ag_{1.6}$ alloy initially quenched from 1173 K in water at 273 K and then heated.

Table 1
Parameters obtained from Rietveld refinement of the X-ray diffraction pattern in Fig. 3.

Symbols	α	Ag	Ag	$\beta_3(L2_1)$	$\beta_1(DO_3)$	β_{Mn}	T_3	GOF	Rwp
Compounds	Cu	Ag (bcc)	Ag (hcp)	Cu_2AlMn	Cu_3Al	Mn	Cu_3AlMn_2		
at.%	71.5	3.2	3.7	6.7	8.0	4.5	2.5	1.6	2.6
Space Groups	*Fm*-3*m*	*Fm*-3*m*	*P*63/*mmc*	*Fm*-3*m*	*Fm*-3*m*	$P4_132$	*Fd*-3*mS*		

and β_{Mn} stable phases and $\beta(A2) \rightarrow \beta_3(L2_1)_{ferromagnetic} \rightarrow \beta_1(DO_3)$ ordering reactions. This thermal event is shifted to higher temperatures when the heating rate is increased up to 10 K/min, suggesting the dominance of diffusive processes. For heating rates higher than 10 K/min the peak temperature is stabilized, thus indicating a limit for the diffusivity increase of Cu atoms in the $Cu_{72.9}Al_{15.0}Mn_{10.5}Ag_{1.6}$ alloy during the bainite formation and the dominance of short-range ordering processes. The exothermic event P_2 at about 650 K is associated with the α-rich Cu phase precipitation from bainitic phase decomposition. This justifies the additional decrease on the alloy microhardness from 723 K in Fig. 1b, since the α-Cu rich phase is softer than the bainite. The endothermic event P_3 at about 760 K is ascribed to the $\beta_1(DO_3)+T_3$-$Cu_3AlMn_2+Ag_{ppt}+\alpha+\beta_{Mn} \rightarrow \beta_2(B2)+T_3$-$Cu_3AlMn_2+\alpha$ reaction, and P_4 at about 780 K is related to the T_3-$Cu_3AlMn_2+\alpha+\beta_2(B2) \rightarrow \beta(A2)+\alpha$ transition [4]. These transitions are not shifted to higher temperatures when the heating rate is elevated, suggesting that the short-range ordering reactions are dominant in these temperature intervals. Fig. 4 shows the phase stability range proposed for the $Cu_{72.9}Al_{15.0}Mn_{10.5}Ag_{1.6}$ alloy initially quenched from 1173 K in water at 273 K during heating.

As seen above, different phase transitions are observed during heating of the $Cu_{72.9}Al_{15.0}Mn_{10.5}Ag_{1.6}$ alloy initially quenched from 1173 K in water at 273 K, but the bainitic phase is responsible for the microhardness increase in this alloy [1,11]. Therefore, the alloy microhardness can be monitored during aging at constant temperatures and the result could be used for the calculation of the activation energy for the bainitic phase precipitation in the $Cu_{72.9}Al_{15.0}Mn_{10.5}Ag_{1.6}$ alloy.

Fig. 5a,b shows the microhardness change measurements with aging time obtained for the $Cu_{72.9}Al_{15.0}Mn_{10.5}Ag_{1.6}$ alloy initially quenched from 1173 K in water at 273 K and then aged at 573 K and 673 K. Other curves were obtained at the aging temperatures of 523, 623 and 723 K. The aging curves of the Fig. 5a,b shows an incubation period, during which the hardness values are practically constant and then there is a hardness increase followed by a stabilization period and after there is a hardness decrease followed by a final stabilization period. The microhardness maximum reached is around the same value found in Fig. 1b for the hardness peak at 523 K, suggesting that age hardening in this alloy is also due to the bainite growth, as shown by the optical micrographs in Fig. 6 (see marked region by circle). At the final stages of the bainitic phase precipitation the formation of the T_3-Cu_3AlMn_2, α and β_{Mn} phases occurs together with the precipitation of Ag and ordering reactions, but the effect of the bainite formation on the microhardness values is dominant. In the optical micrographs in Fig. 6 it is possible to confirm that during aging the hardness increase is mainly due to bainitic precipitation. Fig. 5c shows the magnetization curves vs applied field obtained at 300 K from samples aged at 673 K in different aging times. In these curves one can observed that the magnetization is increased up to 20 min and then it decreases at 60 min and 300 min, thus reaching values close to those initials. These results suggest that on aging the $\beta(A2) \rightarrow \beta_3(L2_1)_{ferromagnetic} \rightarrow \beta_1(DO_3)$ ordering reactions begin

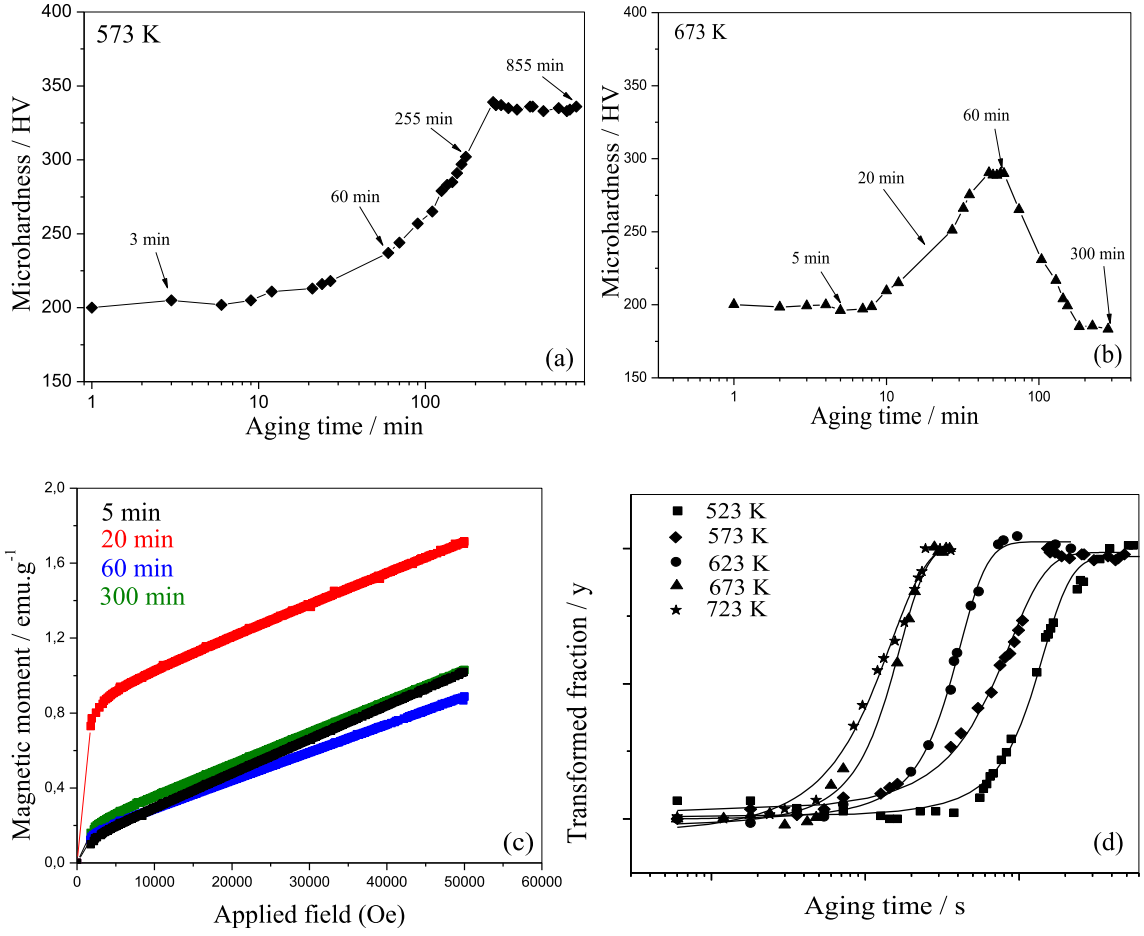

Fig. 5. Microhardness change measurements with aging time at (a) 573 K and (b) 673 K. (c) Magnetization with applied field measurements obtained at 300 K for sample aged at 673 K in different times. (d) Transformed fraction change with aging time obtained from microhardness change measurements with aging time.

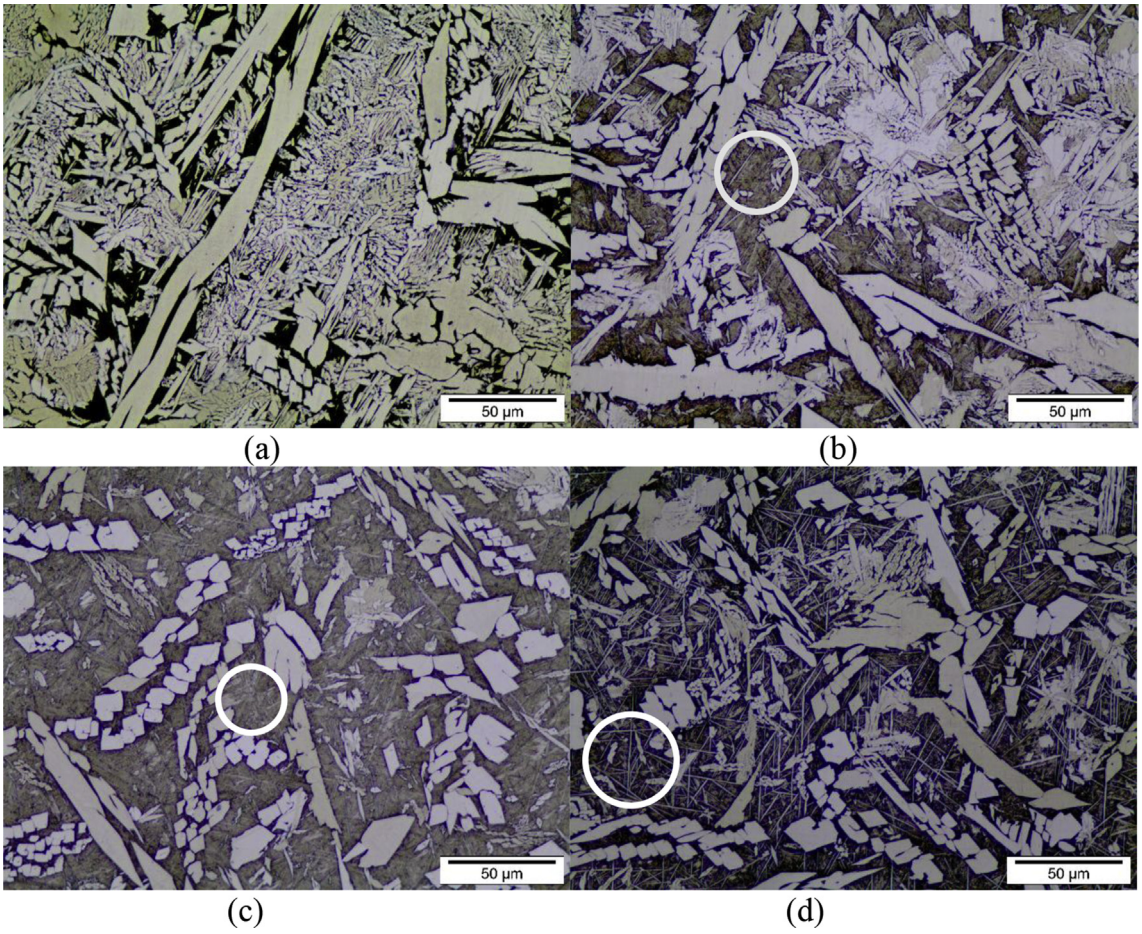

Fig. 6. Optical micrographs obtained for the samples initially quenched from 1173 K in water at 273 K and then aged at 573 K for (a) 3 min, (b) 60 min, (c) 255 min and (c) 805 min.

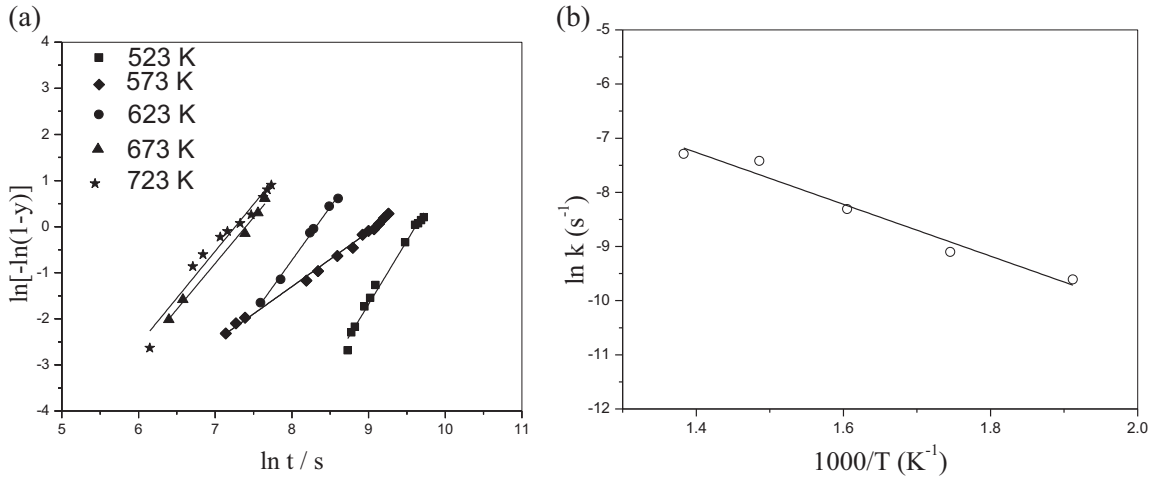

Fig. 7. (a) Plots of ln[-ln(1-y)] vs. ln t and (b) ln k vs. ln1/T.

before the formation of the T_3-Cu_3AlMn_2, α and β_{Mn} phases. Hence, the β(A2) phase is ordered, producing the ferromagnetic $\beta_3(L2_1)$ phase up to 20 min, and then this latter forms the paramagnetic $\beta_1(DO_3)$ phase.

Plots of transformed fraction change with aging time were obtained to study the isothermal aging kinetics of bainitic phase precipitation. Fig. 5d shows these plots and the curves profile suggests that this precipitation is associated with a nucleation and growth process, which may be described by the Johnson-Mehl-Avrami-Kolmogorov (JMAK) equation [1] .

$$y = 1 - \exp\left[-(kt)^n\right] \quad (1)$$

which may be rewritten in the form.

Table 2
Data obtained for the studied alloy using equation (1).

T (K)	523		573		623		673		723		Ea/(kJ mol^{-1})
Parameters	n	k/(s^{-1})	n	k/(s^{-1})	n	k/(s^{-1})	n	k/(s^{-1})	n	k/(s^{-1})	(39.8 ± 3.8)
Values	2.5	6.69×10^{-5}	1.7	1.18×10^{-4}	2.3	2.47×10^{-4}	2.0	6.02×10^{-4}	2.4	6.93×10^{-4}	

$$\ln[-\ln(1-y)] = n \ln t + n \ln k \quad (2)$$

Fig. 7a shows the plots of *ln [−ln (1−y)] vs. ln t* and Table 2 shows the values of n and k obtained from these ones. The n values obtained from the linear fit of the JMAK equation indicate that all the reactional processes associated with alloy aging correspond to diffusional controlled growth with decreasing nucleation rate [12].

The constant k in Eq. (1) can be described by the Arrhenius equation:

$$k = k_0 \exp(-E_a/RT) \quad (3)$$

where k_0 is the pre-exponential factor, E the activation energy for the process and R is the gas constant. Fig. 7b shows the plot of ln$k$ versus the inverse of absolute temperature, for the k values in Table 2. The activation energy value obtained from the slope of the straight line in this figure is $E = 39.8 \pm 3.8$ kJ mol^{-1}.

This activation energy value is lower than that obtained for bainitic precipitation in the $Cu_{71.9}Al_{16.6}Mn_{9.3}Ni_2B_{0.2}$ alloy (E = ~60 kJ mol^{-1}) [1] and in the Cu-9wt.%Al-4wt.%Mn-5wt.%Ag alloy (E = 59 ± 3 kJ mol^{-1}) [13] and it is also lower than those obtained for Ag precipitation in Cu-Al-Ag alloys [14]. This may be due to the occurrence of a diffusion process disturbed by the presence of Ag. In the $Cu_{72.9}Al_{15.0}Mn_{10.5}Ag_{1.6}$ alloy here considered the growth of bainite plates is due to interface diffusion along the phase boundaries between the bainitic and the β(A2) phase. It is important to notice that the precipitation of Ag occurs after the bainitic phase formation. This latter is saturated of silver when bainitic precipitation is started. The presence of Ag may be enhancing the Cu diffusion process, due to a higher bainitic saturation resulting from Ag dissolution on the matrix, thus decreasing the activation energy for the bainitic precipitation.

3. Conclusions

The results indicated that during heating of the $Cu_{72.9}Al_{15.0}Mn_{10.5}Ag_{1.6}$ alloy initially quenched from 1173 K in water at 273 K the formation of the ferromagnetic $\beta_3(L2_1)$ phase occurs in the temperature range from 500 to 560 K. During aging of the $Cu_{72.9}Al_{15.0}Mn_{10.5}Ag_{1.6}$ alloy the bainitic precipitation is dominant on the increase of microhardness. It was observed that the presence of Ag modifies the bainitic growth mechanism. The kinetic parameters indicated that the growth of bainite plates is due to interface diffusion along the phase boundaries between the bainitic and the β(A2) phase. The presence of Ag may be enhancing the Cu diffusion process, thus causing a decrease in the activation energy value for the bainitic precipitation.

Acknowledgments

The authors thank to FAPESP (Proc. 2011/11041-1) and CNPq (Proc. 484135/2012) for financial support.

References

[1] Y. Sutou, N. Koeda, T. Omori, R. Kainuma, K. Ishida, Effects of ageing on bainitic and thermally induced martensitic transformations in ductile Cu-Al-Mn-based shape memory alloys, Acta Mater. 57 (2009) 5748–5758.
[2] M.L. Castro, R. Romero, Isothermal decomposition of the Cu-22.72Al-3.55Be at.% alloy, Mater. Sci. Eng. A 287 (2000) 66–71.
[3] N. Zárubová, V. Novák, Phase stability of CuAlMn shape memory alloys, Mater. Sci. Eng. A 378 (2004) 216–221.
[4] E. Obradó, C. Frontera, L. Manõsa, A. Planes, Order–disorder transitions of Cu-Al-Mn shape-memory alloys, Phys. Rev. B 58 (21) (1998) 14245–14255.
[5] V. Asanovic, K. Delijic, N. Jaukovic, A study of transformations of β-phase in Cu-Zn-Al shape memory alloys, Scr. Mater. 58 (2008) 599–601.
[6] R.A.G. Silva, A. Paganotti, A.T. Adorno, C.M.A. Santos, T.M. Carvalho, Precipitation hardening in the Cu-11wt.%Al-10wt.%Mn alloy with Ag addition, J. Alloy.Compd. 643 (2015) S178–S181.
[7] R.A.G. Silva, A. Paganotti, S. Gama, A.T. Adorno, T.M. Carvalho, C.M.A. Santos, Investigation of thermal, mechanical and magnetic behaviors of the Cu-11%Al alloy with Ag and Mn additions, Mater. Charact. 75 (2013) 194–199.
[8] D. Balzar, N.C. Popa, Analyzing microstructure by Rietveld refinement, Rigaku J. 22 (1) (2005) 16–25.
[9] A.A. Coelho, J. Evans, I. Evans, A. Kern, S. Parsons, The TOPAS symbolic computation system, Powder Diffr. 26 (S1) (2011) 22–25.
[10] R. Kainuma, S. Takahashi, K. Ishida, Thermoelastic martensite and shape memory effect in ductile, Metallurgical Mater. Trans. A 27A (1996) 2187–2195.
[11] Y. Sutou, T. Omori, A. Furukawa, Y. Takahashi, R. Kainuma, K. Yamauchi, S. Yamashita, K. Ishida, Development of medical guide wire of Cu-Al-Mn-basesuperelastic alloy with functionally graded characteristics, J. Biomed. Mat. Res. B 69 (2004) 64–69.
[12] J.W. Christian, The Theory of Transformations in Metals and Alloys, Part I: Equilibrium and General Kinetic Theory, second ed., Pergamon Press, Oxford, 1975.
[13] A.T. Adorno, T.M. Carvaho, A.G. Magdalena, C.M.A. Dos Santos, R.A.G. Silva, Bainitic precipitation in the Cu-9wt.%Al-4wt.%Mn5wt.%Ag alloy, J. Alloy. Compd. 615 (2014) S153–S155.
[14] A.T. Adorno, A.G. Magdalena, R.A.G. Silva, Diffusion and interface controlled reactions in α-(Cu-Al-Ag) alloys, J. Alloy. Compd. 441 (2007) 119–123.